Supplementary materials

Supplementary Results

Supplementary Fig. S1. Habitual Foot Strike Angle

Supplementary Table S1. Selected footwear models

Supplementary Table S2. Foot Strike Angle

Supplementary Table S3. Joint Kinematics

Supplementary Table S4. Spatiotemporal Variables

Supplementary Table S5. Ground Reaction Force and Impulse

Supplementary Table S6. Joint Kinetics and Muscle Forces

Supplementary Table S7. Incremental Test Results

Supplementary Video S1. Animated abstract

Supplementary Fig. S1. Habitual Foot Strike Angle

Supplementary Fig. 1 presents the distribution of the habitual foot strike angle (FSA) of all participants measured during the incremental tests. According to the classifications reported in a previous study,[10] the participants can be categorized as follows: six rearfoot strikers, six midfoot strikers, and three forefoot strikers. In our analysis, we treated the habitual FSA as a continuous variable and added it to a linear mixed-model as a covariate rather than using the habitual FSA to categorize the participants into three groups.

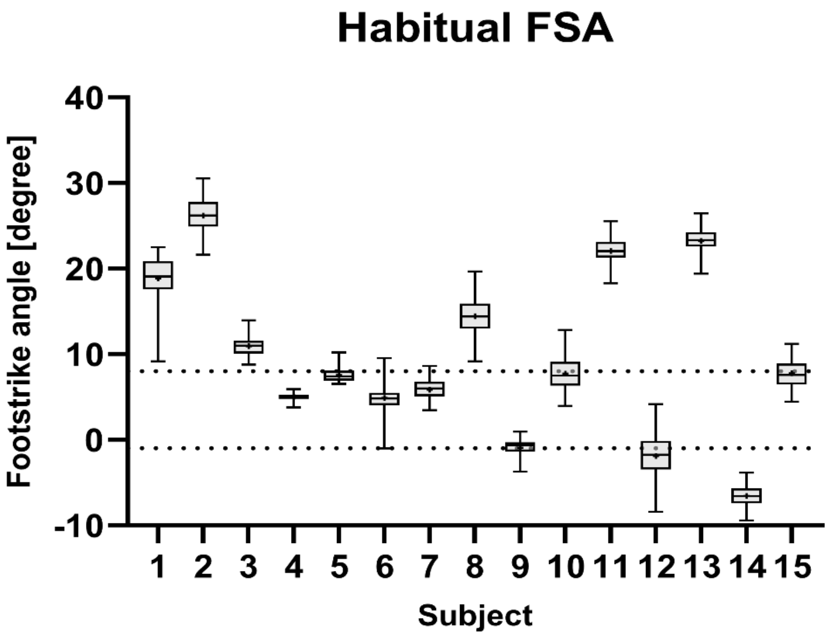

Fig. S1. Distribution of the habitual foot strike angle (FSA) during the incremental test. The median (central line), mean ('·' symbol), first and third quartiles (lower and upper box boundaries), and minimum and maximum values (lower and upper whiskers) of the FSA values are depicted in the box plot. The horizontal dotted lines indicate the FSA criteria used in previous studies classifying runners into rearfoot, midfoot, and forefoot strikers[10].

Supplementary Table S1. Selected footwear models

Evaluation of energy return was conducted by K2 Korea using standardized testing protocols in which compressive force up to 10 kN was applied at a constant displacement rate of 50 mm/min. The minimalist index was determined according to the standardized criteria proposed by Esculier et al[23].

Table S1. Summary of key material and structural properties of selected footwear models

Property	Conventional cushioned shoes (CON)	Technologically advanced running shoes (TARS)	Minimalist shoes (MIN)
Model	Adidas, UltraBoost 20	Nike, Alphafly next%	Asics, SORTIEMAGIC RP5
Mass (g)	310	210	160
Energy Return – Forefoot (%)	78.57	86.26	73.26
Energy Return – Rearfoot (%)	82.56	87.25	73.07
Heel Midsole Height (mm)	22	39	10
Forefoot Midsole Height (mm)	12	35	10
Heel-to-Toe Offset (mm)	10	4	0
Minimalist Index (%)	12	28	76
Midsole Material	Boost™ foam (expanded thermoplastic polyurethane, eTPU)	ZoomX foam (PEBA-based foam) + Carbon Fiber Plate	SOLYTE® (proprietary EVA-blend midsole)

Supplementary Table S2. Foot Strike Angle

Supplementary Table S2 summarizes the results of the linear mixed model analysis. Technologically advanced running shoes (TARS) induce significantly lower FSA than conventional cushioned shoes (CON) ($\beta = -4.174$, $p < 0.05$). In contrast, the FSA induced by minimalist shoes (MIN) is not significantly different from that induced by CON ($p > 0.05$). The intercept represents the estimated average FSA under the CON condition when the habitual FSA is zero. Habitual FSA exerts a significant influence on FSA during running ($\beta = 0.512$, $p < 0.001$), but this effect does not vary across different conditions ($p > 0.05$).

Table S2. Fixed effects estimates (β [95% CI]) from the linear mixed model for foot strike angle (FSA). * $p < 0.05$, ** $p < 0.01$, and *** $p < 0.001$.

Dependent variable	Shoe effect (β_1)		Habitual FSA effect (β_2)	Interaction (β_3)		Intercept (β_0)
	TARS	MIN		TARS: Habitual FSA	MIN: Habitual FSA	
FSA [degree]	-4.174* [-7.372,-0.977]	-2.034 [-4.178,0.109]	0.512*** [0.338,0.686]	-0.096 [-0.335, 0.143]	0.040 [-0.128, 0.192]	-2.038 [-4.364,0.289]

Supplementary Table S3. Joint Kinematics

The results of the linear mixed model analysis indicate several significant effects of shoe conditions and habitual FSA on the joint angles at initial contact (IC) and during the loading response (LR) phase (Supplementary Table 2). The IC ankle plantarflexion angle under the TARS condition is significantly higher than that under the CON condition ($\beta = 6.076$, $p < 0.05$), suggesting that TARS promote a more plantarflexed ankle position at IC, thereby facilitating a more forefoot-oriented landing. In contrast, no significant effect is observed under the MIN condition ($\beta = 1.190$, $p > 0.05$). Similarly, the IC subtalar eversion angle under the TARS condition is significantly higher than that under the CON condition ($\beta = 4.731$, $p < 0.01$), but no significant effect is observed under the MIN condition ($\beta = 2.508$, $p > 0.05$). A significant increase in the hip flexion range ($\beta = 0.959$, $p < 0.01$), and a decrease in the subtalar eversion range ($\beta = -1.808$, $p < 0.05$) compared with those under the CON condition are observed during the LR phase. In contrast, no significant change in these variables is observed under the MIN condition ($p > 0.05$). Significant interactions are observed between the habitual FSA and shoe conditions. TARS tend to reduce the hip flexion range during the LR phase for runners with high habitual FSA ($\beta = -0.132$, $p < 0.001$). Similarly, MIN induce relative decreases in the subtalar eversion range of motion during the LR phase for runners with high habitual FSA ($\beta = -0.139$, $p < 0.05$).

Table S3. Fixed effects estimates (β [95% CI]) from the linear mixed model for joint angles (degree) at initial contact (IC) and loading response (LR). The table includes statistical results for the effects of habitual foot strike angle (FSA), shoe conditions, and their interaction. * $p < 0.05$, ** $p < 0.01$, and *** $p < 0.001$.

Dependent variable	Shoe effect (β_1)		Habitual FSA effect (β_2)	Interaction (β_3)		Intercept (β_0)
	TARS	MIN		TARS: Habitual FSA	MIN: Habitual FSA	
IC Hip flexion	-0.106 [-1.183,0.971]	0.004 [-1.071,1.079]	0.201*** [0.125,0.276]	-0.005 [-0.085,0.074]	-0.005 [-0.085,0.074]	28.848*** [27.830,29.865]
IC Hip abduction	0.119 [-0.982,1.22]	0.248 [-0.851,1.347]	0.106** [0.029,0.183]	0.026 [-0.055,0.108]	0.024 [-0.057,0.105]	-3.475*** [-4.515,-2.434]
IC Hip external rotation	1.162 [-0.178,2.502]	-1.131 [-2.468,0.207]	0.133** [0.040,0.227]	-0.066 [-0.165,0.033]	0.072 [-0.027,0.171]	3.644*** [2.378,4.91]

IC Knee flexion	-0.139 [-1.733,1.455]	-0.854 [-2.445,0.737]	-0.236*** [-0.348,-0.125]	0.071 [-0.047,0.189]	0.008 [-0.109,0.126]	31.249*** [29.743,32.755]
IC Ankle plantarflexion	6.260*** [4.909,7.610]	1.242 [-0.106,2.589]	-0.112* [-0.207,-0.018]	-0.216*** [-0.316,-0.116]	0.054 [-0.046,0.153]	0.147 [-1.129,1.423]
IC Subtalar eversion	4.825*** [3.129,6.521]	2.570** [0.877,4.263]	-0.285*** [-0.403,-0.166]	-0.062 [-0.188,0.063]	-0.009 [-0.134,0.116]	1.659* [0.056,3.262]
LR Hip flexion range	0.841 [-0.657,2.34]	0.343 [-1.153,1.839]	-0.001 [-0.106,0.104]	-0.125* [-0.236,-0.015]	-0.009 [-0.119,0.101]	13.044*** [11.628,14.461]
LR Hip abduction range	0.160 [-1.148,1.469]	0.884 [-0.029,1.797]	0.055 [-0.051,0.161]	0.024 [-0.074,0.121]	-0.004 [-0.072,0.064]	3.025** [1.606,4.444]
LR Hip external rotation range	0.534 [-0.679,1.746]	0.285 [-0.451,1.02]	0.070 [-0.004,0.144]	-0.006 [-0.096,0.085]	-0.004 [-0.058,0.051]	1.537** [0.543,2.53]
LR Knee flexion range	-1.155 [-2.792,0.482]	-0.513 [-2.147,1.121]	0.190** [0.075,0.304]	-0.036 [-0.157,0.085]	-0.009 [-0.130,0.111]	20.079*** [18.532,21.625]
LR Ankle plantarflexion range	1.408* [0.212,2.605]	0.503 [-0.691,1.697]	-0.085* [-0.169,-0.001]	-0.068 [-0.156,0.021]	0.068 [-0.020,0.157]	18.434*** [17.303,19.564]
LR Subtalar eversion range	-1.808* [-3.043,-0.574]	0.212 [-1.129,1.552]	0.068 [-0.162,0.297]	-0.030 [-0.121,0.062]	-0.139* [-0.238,-0.039]	7.620*** [4.547,10.693]

Supplementary Table S4. Spatiotemporal Variables

The results of the linear mixed model analysis indicate that MIN exert significant effects on some spatiotemporal variables (Supplementary Table 3). Significant increases in step frequency ($\beta = 2.984$, $p < 0.01$), dimensionless step frequency ($\beta = 0.406$, $p < 0.05$), step length ($\beta = -0.019$, $p < 0.05$), and normalized step length ($\beta = -0.023$, $p < 0.05$) are observed under the MIN condition compared with those under the CON condition. However, no significant effect is observed on these variables under the TARS condition ($p > 0.05$). Habitual FSA exerts a significant effect on the center of mass (CoM)-ankle horizontal distance ($\beta = 0.001$, $p < 0.01$), normalized CoM-ankle horizontal distance ($\beta = 0.001$, $p < 0.01$), knee-ankle horizontal distance ($\beta = 0.001$, $p < 0.001$), and normalized knee-ankle horizontal distance ($\beta = 0.002$, $p < 0.001$) at IC. A variation in this effect is not observed across shoe conditions ($p > 0.05$). This finding indicates that runners with high habitual FSA land with their feet ahead of their CoM positions. Significant interactions between habitual FSA and the TARS condition are observed for these four horizontal distance-related variables ($\beta = -0.001$, $p < 0.05$). This finding indicates that TARS mitigate the tendency to land with the feet ahead of the body for runners with high habitual FSA.

Table S4. Fixed effects estimates (β [95% CI]) from the linear mixed model for spatiotemporal variables. The table includes statistical results for the effects of habitual foot strike angle (FSA), shoe conditions, and their interaction. The listed horizontal distances between center of mass (CoM) and ankle, and between knee and ankle, and those which are normalized to the leg length are evaluated at initial contact. * $p < 0.05$, ** $p < 0.01$, and *** $p < 0.0001$.

Dependent variable	Shoe effect (β_1)		Habitual FSA effect (β_2)	Interaction (β_3)		Intercept (β_0)
	TARS	MIN		TARS: Habitual FSA	MIN: Habitual FSA	
Step frequency [steps min^{-1}]	1.982 [-0.037,4.002]	2.984** [0.964,5.004]	-0.469 [-1.233,0.296]	-0.074 [-0.224,0.076]	-0.049 [-0.199,0.102]	182.946*** [172.653,193.24]
Dimensionless step frequency	0.297 [-0.002,0.596]	0.406* [0.107,0.705]	-0.070 [-0.17,0.029]	-0.011 [-0.033,0.012]	-0.001 [-0.023,0.021]	26.406*** [25.064,27.747]
Contact time [s]	-0.002 [-0.006,0.001]	-0.001 [-0.005,0.002]	0.001 [0.000,0.002]	0.000 [0.000,0.000]	0.000 [0.000,0.001]	0.232*** [0.219,0.245]
Step length [m]	-0.012 [-0.026,0.002]	-0.019* [-0.033,-0.005]	-0.001 [-0.007,0.005]	0.001 [-0.001,0.002]	0.000 [-0.001,0.001]	1.330*** [1.250,1.410]

Normalized step length	-0.019 [-0.039,0.001]	-0.023* [-0.043,-0.003]	-0.001 [-0.009,0.007]	0.001 [-0.001,0.002]	0.000 [-0.002,0.001]	1.627*** [1.518,1.736]
Horizontal CoM – ankle distance [m]	-0.003 [-0.013,0.008]	0.002 [-0.009,0.012]	0.001** [0.000,0.002]	-0.001* [-0.002,0.000]	0.000 [-0.001,0.001]	0.179*** [0.169,0.188]
Normalized horizontal CoM – ankle distance	-0.004 [-0.017,0.009]	0.003 [-0.010,0.015]	0.001** [0.001,0.002]	-0.001* [-0.001,0.000]	0.000 [-0.001,0.001]	0.218*** [0.207,0.230]
Horizontal knee – ankle distance [m]	-0.001 [-0.010,0.008]	0.003 [-0.006,0.012]	0.001*** [0.001,0.002]	-0.001* [-0.001,0.000]	0.000 [-0.001,0.001]	0.012** [0.004,0.020]
Normalized horizontal knee – ankle distance	-0.002 [-0.013,0.009]	0.004 [-0.007,0.015]	0.002*** [0.001,0.002]	-0.001* [-0.002,0.000]	0.000 [-0.001,0.001]	0.015** [0.004,0.025]

Supplementary Table S5. Ground Reaction Force and Impulse

MIN significantly decrease the peak vertical ground reaction force (GRF) compared with CON (β = -0.088, $p < 0.001$, Supplementary Table 4). In contrast, no statistically significant difference in this variable between the CON and TARS conditions is observed (β = 0.010, $p > 0.05$). Habitual FSA exhibits no significant main effect on the peak vertical GRF, but a significant interaction is observed between habitual FSA and the MIN condition (β = 0.004, $p < 0.05$). The positive β_3 value for this interaction suggests that the effect of MIN on reducing the peak vertical GRF diminishes as the habitual FSA increases; MIN are effective in reducing the peak vertical GRF in runners with low habitual FSA, but the efficacy becomes less pronounced when runners have high habitual FSA. For propulsion impulse, the result shows a significant interaction between habitual FSA and the MIN condition (β = 0.001, $p < 0.05$), indicating that the effect of MIN on propulsion impulse also depends on the habitual FSA of the runner.

Table S5. Fixed effects estimates (β [95% CI]) from the linear mixed model for peak vertical ground reaction force (GRF) and impulses. The table includes statistical results for the effects of habitual foot strike angle (FSA), shoe conditions, and their interaction. * $p < 0.05$, ** $p < 0.01$, and *** $p < 0.001$.

Dependent variable	Shoe effect (β_1)		Habitual FSA effect (β_2)	Interaction (β_3)		Intercept (β_0)
	TARS	MIN		TARS: Habitual FSA	MIN: Habitual FSA	
Peak vertical GRF [BW][a]	0.010 [-0.041,0.06]	-0.088*** [-0.127,-0.048]	-0.004 [-0.017,0.008]	0.000 [-0.004,0.004]	0.004* [0.001,0.007]	2.546*** [2.376,2.716]
Braking impulse [BW·s]	0.015 [-0.002,0.033]	-0.012 [-0.025,0.002]	0.000 [-0.002,0.002]	-0.001 [-0.003,0.000]	0.000 [-0.001,0.001]	-0.345*** [-0.372,-0.318]
Propulsion impulse [BW·s]	-0.007 [-0.025,0.01]	-0.003 [-0.012,0.005]	-0.001 [-0.002,0.001]	0.000 [-0.001,0.002]	0.001* [0.000,0.001]	0.347*** [0.328,0.366]

[a] BW: body weight

Supplementary Table S6. Joint Kinetics and Muscle Forces

TARS significantly reduce the peak resultant ankle joint reaction force (JRF) compared with CON (β = -1.835, $p < 0.01$). In contrast, MIN significantly increase the peak resultant ankle JRF compared with CON (β = 3.074, $p < 0.001$). Habitual FSA exhibits significant main effects, with higher values being associated with lower peak resultant knee JRF (β = -0.136, $p < 0.001$) and ankle JRF (β = -0.192, $p < 0.001$). Significant interactions are also observed between habitual FSA and the TARS and MIN conditions for peak resultant knee JRF (β = 0.077, $p < 0.01$; and β = 0.085, $p < 0.01$, respectively). This finding indicates that TARS and MIN attenuate the reduction in peak resultant knee JRF when runners have high habitual FSA, and the attenuation effect is stronger under the MIN condition. Similarly, a significant interaction is observed between habitual FSA and the TARS condition for peak resultant ankle JRF (β = 0.107, $p < 0.05$); although high habitual FSA and TARS independently reduce peak resultant ankle JRF, the combination of high habitual FSA and TARS can attenuate the reduction in the peak resultant ankle JRF.

MIN significantly increase the peak gastrocnemius force (β = 0.936, $p < 0.01$) and peak soleus force (β = 1.51, $p < 0.001$) compared with CON. In contrast, TARS significantly reduce the peak soleus force (β = -1.096, $p < 0.001$) and peak peroneus longus force (β = -0.433, $p < 0.01$) compared with CON. Higher habitual FSA exhibits significant associations with significantly increased peak gluteus maximus force (β = 0.033, $p < 0.01$), decreased peak gastrocnemius force (β = -0.081, $p < 0.001$), and decreased peak soleus force (β = -0.046, $p < 0.05$). Notably, significant interactions are observed between habitual FSA and the TARS and MIN conditions for peak gastrocnemius force (β = 0.057, $p < 0.01$; β = 0.065, $p < 0.01$, respectively). This finding indicates that a higher value of habitual FSA is associated with a greater increase in the peak gastrocnemius force under the MIN and TARS conditions, with a stronger effect observed under the MIN condition. Although a significant increase in the peak soleus force is observed under the MIN condition, a significant interaction with habitual FSA (β = -0.057, $p < 0.05$) suggests that this increase can be attenuated in runners with high habitual FSA. In contrast, although a significant decrease in the peak soleus force is observed under the TARS condition, a significant interaction with habitual FSA (β = 0.058, $p < 0.01$) suggests that this reduction effect can decrease in runners with high habitual FSA.

Habitual FSA exerts a significant main effect on the total energy absorption (β = 0.009, p <

0.01). In addition, significant interactions are observed between habitual FSA and the TARS (β = -0.006, $p < 0.05$) and MIN (β = -0.006, $p < 0.05$) conditions for the total absorbed energy. Regarding the percent contribution of each joint to the total energy, habitual FSA exhibits significant effects on the contribution of the hip joint to the energy generation (β = 0.273, $p < 0.01$), the contribution of the knee joint to the energy absorption (β = 0.350, $p < 0.05$), the contribution of the ankle joint to the energy absorption (β = -0.574, $p < 0.001$), and the contribution of the ankle joint to the energy generation (β = -0.370, $p < 0.001$). TARS significantly increase the contribution of the ankle joint to the energy absorption compared with CON (β = 4.298, $p < 0.05$). In contrast, MIN significantly increase the contribution of the ankle joint to the energy generation (β = 3.193, $p < 0.05$) and decrease the contribution of the subtalar joint to the energy generation (β = -1.450, $p < 0.05$) compared with CON. A significant interaction is observed between habitual FSA and the TARS condition for the ankle joint contribution to the energy generation (β = 0.230, $p < 0.05$). Regarding mechanical energy, significant reductions in the knee joint energy generation (β = -0.035, $p < 0.01$) and subtalar joint energy generation (β = -0.024, $p < 0.05$) are observed under the MIN condition compared with those observed under the CON condition. This finding indicates that the energy generated by the knee and subtalar joints during the propulsion phase decreases while running under the MIN condition. Habitual FSA exerts significant main effects on the hip joint energy absorption (β = -0.005, $p < 0.01$), hip joint energy generation (β = 0.004, $p < 0.01$), knee joint energy absorption (β = -0.006, $p < 0.001$), and ankle joint energy absorption (β = 0.003, $p < 0.05$).

Regarding peak joint powers, significant reductions in the peak knee joint power generation are observed under the TARS (β = -0.498, $p < 0.05$) and MIN (β = -0.725, $p < 0.01$) conditions compared with the peak knee joint power generation under the CON condition, with a larger reduction under the MIN condition. A significant decrease in the peak subtalar joint power generation is observed under the MIN condition (β = -0.535, $p < 0.05$). Significant interactions are observed between habitual FSA and the MIN condition for peak hip joint power absorption (β = 0.038, $p < 0.001$) and for peak hip joint power generation (β = -0.036, $p < 0.05$), indicating that higher habitual FSA is associated with increased hip joint power absorption during the landing phase and decreased hip joint power generation during the propulsion phase under the MIN condition. Habitual FSA also exhibits significant main effects on the peak knee joint power absorption (β = -0.112, $p < 0.001$), peak ankle joint power absorption (β = 0.059, p <

0.01), and peak ankle joint power generation (β = -0.235, $p < 0.01$).

Table S6. Fixed effects estimates (β [95% CI]) from the linear mixed model for resultant joint reaction forces (JRF) and muscle forces normalized to body weight (BW), total absorbed and generated mechanical energy per body mass (J·kg-1), percent contribution of each joint to the total energy (%), and absorbed and generated powers per body mass (W·kg-1). The table includes statistical results for the effects of habitual foot strike angle (FSA), shoe conditions, and their interaction. * $p < 0.05$, ** $p < 0.01$, and *** $p < 0.001$.

Dependent variable	Shoe effect (β_1)		Habitual FSA effect (β_2)	Interaction (β_3)		Intercept (β_0)
	TARS	MIN		TARS: Habitual FSA	MIN: Habitual FSA	
Peak resultant hip JRF	-1.462 [-3.243,0.32]	-0.943 [-2.722,0.835]	-0.119 [-0.243,0.006]	0.065 [-0.067,0.197]	0.035 [-0.097,0.166]	12.843*** [11.159,14.526]
Peak resultant knee JRF	-0.679 [-1.426,0.067]	0.626 [-0.119,1.372]	-0.136*** [-0.188,-0.083]	0.077** [0.022,0.133]	0.085** [0.03,0.14]	15.806*** [15.101,16.512]
Peak resultant ankle JRF	-1.835** [-3.096,-0.573]	3.074*** [1.815,4.333]	-0.192*** [-0.28,-0.103]	0.107* [0.014,0.201]	0.02 [-0.073,0.113]	19.893*** [18.701,21.086]
Peak gluteus maximus force	0.073 [-0.224,0.370]	0.174 [-0.122,0.471]	0.033** [0.012,0.054]	0.011 [-0.011,0.033]	-0.016 [-0.038,0.006]	1.446*** [1.165,1.727]
Peak rectus femoris force	-0.062 [-0.219,0.095]	-0.005 [-0.162,0.152]	-0.006 [-0.017,0.005]	0.005 [-0.006,0.017]	0.009 [-0.002,0.021]	1.338*** [1.189,1.486]
Peak vastus force	-0.617 [-1.332,0.098]	-0.300 [-1.014,0.414]	-0.024 [-0.074,0.026]	0.017 [-0.036,0.070]	0.001 [-0.052,0.053]	10.242*** [9.566,10.918]
Peak gastrocnemius force	-0.326 [-0.885,0.233]	0.936** [0.378,1.493]	-0.081*** [-0.120,-0.042]	0.057** [0.016,0.098]	0.065** [0.024,0.106]	6.920*** [6.392,7.448]
Peak soleus force	-1.096*** [-1.683,-0.508]	1.510*** [0.924,2.097]	-0.046* [-0.087,-0.005]	0.058** [0.015,0.101]	-0.057* [-0.100,-0.013]	7.604*** [7.048,8.159]
Peak tibialis anterior force	-0.193 [-0.393,0.007]	0.055 [-0.145,0.255]	0.005 [-0.009,0.019]	0.002 [-0.012,0.017]	-0.001 [-0.016,0.013]	0.429*** [0.240,0.618]
Peak peroneus longus force	-0.433** [-0.722,-0.144]	0.064 [-0.225,0.352]	-0.017 [-0.037,0.003]	0.006 [-0.016,0.027]	0.004 [-0.018,0.025]	2.815*** [2.542,3.088]
Total energy absorption	-0.003 [-0.081,0.075]	0.025 [-0.053,0.102]	0.009** [0.003,0.014]	-0.006* [-0.012,0.000]	-0.006* [-0.012,0.001]	0.911*** [0.837,0.984]
Total energy generation	-0.063 [-0.173,0.046]	-0.018 [-0.127,0.091]	0.001 [-0.007,0.008]	0.003 [-0.005,0.011]	0.001 [-0.007,0.009]	1.544*** [1.441,1.647]
Hip joint contribution to absorption	-0.188 [-4.031,3.656]	2.012 [-1.824,5.848]	0.176 [-0.093,0.445]	0.097 [-0.187,0.381]	-0.104 [-0.387,0.179]	23.495*** [19.863,27.127]
Hip joint contribution to generation	1.965 [-0.624,4.555]	0.116 [-2.469,2.7]	0.273** [0.091,0.454]	-0.110 [-0.302,0.081]	-0.070 [-0.261,0.121]	20.714*** [18.267,23.161]
Knee joint contribution to absorption	-3.045 [-7.064,0.975]	-3.338 [-7.350,0.674]	0.350* [0.068,0.631]	0.099 [-0.198,0.396]	0.094 [-0.202,0.390]	20.937*** [17.139,24.735]
Knee joint contribution to generation	-0.854 [-3.042,1.334]	-1.859 [-4.043,0.326]	0.071 [-0.083,0.224]	-0.049 [-0.211,0.113]	-0.020 [-0.181,0.141]	12.319*** [10.251,14.387]
Ankle joint contribution to absorption	4.298* [0.603,7.993]	2.112 [-1.576,5.800]	-0.574*** [-0.833,-0.315]	-0.123 [-0.396,0.150]	0.069 [-0.203,0.341]	48.971*** [45.479,52.462]

Ankle joint contribution to generation	-0.567 [-3.511,2.377]	3.193* [0.255,6.132]	-0.370*** [-0.576,-0.164]	0.230* [0.012,0.448]	0.104 [-0.113,0.321]	62.800*** [60.018,65.582]
Subtalar joint contribution to absorption	-1.066 [-2.824,0.692]	-0.786 [-2.541,0.968]	0.049 [-0.074,0.172]	-0.072 [-0.202,0.058]	-0.059 [-0.189,0.070]	6.598*** [4.936,8.259]
Subtalar joint contribution to generation	-0.545 [-1.85,0.761]	-1.450* [-2.753,-0.147]	0.027 [-0.065,0.118]	-0.071 [-0.167,0.026]	-0.014 [-0.11,0.082]	4.167*** [2.933,5.400]
Peak hip joint power absorption	0.027 [-0.236,0.290]	-0.188 [-0.450,0.075]	-0.016 [-0.035,0.002]	0.005 [-0.014,0.025]	0.038*** [0.018,0.057]	-4.325*** [-4.573,-4.077]
Peak hip joint power generation	0.197 [-0.295,0.69]	-0.027 [-0.519,0.464]	0.029 [-0.005,0.064]	-0.007 [-0.043,0.029]	-0.036* [-0.073,0]	3.942*** [3.476,4.407]
Peak knee joint power absorption	0.000 [-0.802,0.802]	0.369 [-0.431,1.17]	-0.112*** [-0.168,-0.056]	0.057 [-0.002,0.116]	0.033 [-0.026,0.092]	-4.506*** [-5.263,-3.748]
Peak knee joint power generation	-0.498* [-0.969,-0.026]	-0.725** [-1.196,-0.254]	0.005 [-0.028,0.038]	0.005 [-0.030,0.040]	0.013 [-0.021,0.048]	4.147*** [3.701,4.593]
Peak ankle joint power absorption	-0.253 [-0.856,0.349]	-0.453 [-1.054,0.149]	0.059** [0.017,0.101]	0.033 [-0.012,0.077]	0.007 [-0.038,0.051]	-8.584*** [-9.154,-8.015]
Peak ankle joint power generation	-1.886 [-4.077,0.305]	0.135 [-2.051,2.322]	-0.235** [-0.388,-0.082]	0.161 [-0.001,0.323]	0.114 [-0.048,0.275]	21.484*** [19.414,23.555]
Peak subtalar joint power absorption	0.112 [-0.162,0.386]	0.091 [-0.182,0.364]	-0.008 [-0.027,0.011]	0.014 [-0.006,0.034]	0.011 [-0.009,0.031]	-0.894*** [-1.153,-0.635]
Peak subtalar joint power generation	-0.221 [-0.643,0.2]	-0.535* [-0.956,-0.114]	0.013 [-0.016,0.043]	-0.026 [-0.057,0.006]	-0.010 [-0.041,0.021]	1.745*** [1.347,2.143]

Supplementary Table S7. Incremental Test Results

Supplementary Table 6 summarizes the results of the incremental treadmill test performed prior to the main experiment. For each participant, the ventilatory threshold (VT) speed used to determine submaximal test intensities and the peak oxygen uptake (VO_2 peak) are listed.

Table S7. Incremental test results: peak VO_2 and ventilatory threshold speeds for each participant.

Participant ID	VO_{2peak}/kg (ml/kg/min)	VT Speed (m/s)	HR at VO_{2peak} (bpm)
P01	65.82	3.75	180
P02	52.97	3.55	188
P03	53.51	3.82	188
P04	60.72	4.29	194
P05	60.48	3.76	198
P06	64.83	4.00	196
P07	62.81	4.29	197
P08	65.34	4.00	193
P09	46.77	3.76	188
P10	56.26	4.07	193
P11	53.57	4.07	193
P12	49.95	3.82	193
P13	51.09	3.31	196
P14	45.43	4.06	194
P15	59.54	4.06	195

Supplementary Video S1. Animated abstract

This video illustrates the differences in running biomechanics induced by three distinct shoe conditions for a representative habitual rearfoot strike runner. It begins by showing the foot strike angle in the sagittal plane and providing a visual comparison. The video progresses to present selected results of the inverse dynamic analysis; the effects of shoe conditions on the estimated peak resultant ankle joint reaction force and peak soleus force are shown.